



Facile bimetallic co-amplified electrochemical sensor for folic acid sensing based on CoNPs and CuNPs

Zhen-Fan Zhou¹ · Xiao-Zhen Feng¹ · Tao Zhan¹ · Guo-Cheng Han¹ · Zhencheng Chen¹ · Heinz-Bernhard Kraatz²

Received: 22 June 2022 / Revised: 18 July 2022 / Accepted: 19 July 2022 / Published online: 5 August 2022
© Springer-Verlag GmbH Germany, part of Springer Nature 2022

Abstract

Folic acid (FA) is essential for human health, particularly for pregnant women and infants. In this work, a glassy carbon electrode (GCE) was modified by a bimetallic layer of Cu/Co nanoparticles (CuNPs/CoNPs) as a synergistic amplification element by simple step-by-step electrodeposition, and was used for sensitive detection of FA. The proposed CuNPs/CoNPs/GCE sensor was characterized by differential pulse voltammetry (DPV), electrochemical impedance spectroscopy (EIS) and field emission scanning electron microscopy (FESEM). Then, under optimal conditions, a linear relationship was obtained in the wide range of 110.00–1750.00 μM for the detection of FA with a limit of detection (LOD) of 34.79 μM ($S/N=3$). The sensitivity was calculated as 0.096 $\mu\text{A } \mu\text{M}^{-1} \text{ cm}^{-2}$. Some interfering compounds including glucose (Glc), biotin, dopamine (DA), and glutamic acid (Glu) showed little effect on the detection of FA by amperometry (*i-t*). Finally, the average recovery obtained was in a range of 91.77–110.06%, with a relative standard deviation (RSD) less than 8.00% in FA tablets, indicating that the proposed sensor can accurately and effectively detect the FA content in FA tablets.

Keywords Bimetallic layer Cu/Co nanoparticles · Synergistic amplification · Electrodeposition · Folic acid · Electrochemical sensor

Introduction

Folic acid (FA), generally known as vitamin B9, is a water-soluble vitamin found in various vegetables, fruits, and nutritional supplements [1]. As a coenzyme, it plays a vital role in the synthesis of DNA, RNA, and amino acids [2]. It has been reported that 0.4 mg FA per day is required for pregnant women [3]. Folate deficiency can result in major

consequences such as megaloblastic anemia [4], cardiovascular disease [5], Alzheimer's disease [6], and fetal malformation [7]. Excessive levels of FA intake, however, may result in various health risks [8], such as masking the signs of vitamin B12 insufficiency, abnormal neural development, and colorectal cancer. Consequently, the rapid and accurate detection of FA in food and medicine is critical.

Various methods including high-performance liquid chromatography (HPLC) [9], fluorescence photometry [10], surface plasmon resonance [11], spectrophotometry [12], and other techniques [13] have been commonly used for FA detection. However, these analytical techniques involve time-consuming processes and high cost, which hinders their application [14]. As an alternative, electrochemical sensors have attracted increasing attention in recent years, owing to their low cost, portability, convenience, and excellent selectivity [15, 16]. For the electrochemical sensor toward FA [17, 18], as reported, the single bond between C(9) and N(10) on FA was oxidized into a double bond in the reaction where two electrons and two protons were transferred [19, 20], as illustrated in Scheme 1.

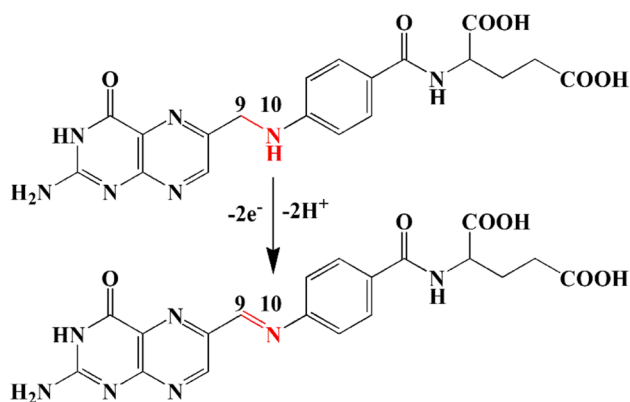
Electroactive materials, such as metal nanoparticles (NPs) [21–24], bioactive substances [25, 26], molecularly

Zhen-Fan Zhou, Xiao-Zhen Feng and Tao Zhan contributed equally to this work.

- ✉ Guo-Cheng Han
hangc81@guet.edu.cn
- ✉ Zhencheng Chen
chenzhch1965@163.com
- ✉ Heinz-Bernhard Kraatz
bernie.kraatz@utoronto.ca

¹ School of Life and Environmental Sciences, Guilin University of Electronic Technology, Guilin 541004, People's Republic of China

² Department of Physical and Environmental Sciences, University of Toronto Scarborough, Toronto, Ontario M1C 1A4, Canada



Scheme 1 Electrochemical oxidation of FA on electrode

imprinted polymers [27, 28], graphene derivatives and nanocomposites [29, 30], are generally modified on bare glassy carbon electrodes (GCEs) to enhance electrochemical response signal. Metal NPs such as cobalt NPs (CoNPs) and copper NPs (CuNPs), in particular, have properties in large specific surface area, excellent catalytic activity, excessive active sites and accelerated electron transfer. For example, Wong et al. [31] synthesized a new dispersion containing carbon black (CB), graphene oxide (GO), CuNPs and poly(3,4-ethylenedioxythiophene)-poly(styrenesulfonate) (PEDOT:PSS) by ultrasonic agitation to construct GO-CB-PEDOT:PSS/GCE for simultaneous sensing of isoproterenol, acetaminophen, FA, propranolol and caffeine by square-wave voltammetry (SWV). Tefera et al. [32] modified pyrrole on GCE by electropolymerization, and then drop-coated CoNPs on it to prepare a CoNPs-polypyrrole composite-modified GCE (CoNPs/PPy/GCE) for the determination of phoxim. This sensor had a wide detection range and high recovery due to the good electrocatalytic activity and high specific surface area of CoNPs.

Likewise, bimetallic NPs have some advantages over monometallic NPs in specific surface area, active sites and impedance [33–35]. For example, Wang et al. [36] reported the synthesis of ZrO_2/ZnO nanocomposites by chemical precipitation and calcination, which were successfully applied for the simultaneous detection of epinephrine, uric acid and FA. Tajik et al. [37] constructed a sensor by modifying a prepared FeO/PPy/Pd nanocomposite on a screen-printed graphite electrode (SPGE), which was applied for the simultaneous determination of FA and methotrexate with an excellent recovery in pharmaceutical and biological samples. These sensors were complex and not easy to fabricate, despite low LOD and sensitive characteristics. Hence, readily available bimetallic NPs are a key point in the FA signal amplification effect.

In this study, a glassy carbon electrode (GCE), individually modified with readily available bioactive substances (thiophene, indole, pyrrole, and dopamine (DA)) and metal NPs (CoNPs, CuNPs, PtNPs, and AgNPs), were compared. Then the order of different modifiers was studied. Differential pulse voltammetry (DPV), electrochemical impedance spectroscopy (EIS), scanning electron microscopy (SEM) and X-ray energy dispersive spectroscopy (EDS) were used to verify the construction of the sensor, respectively. Eventually, CuNPs/CoNPs/GCE was applied to detect FA in FA tablets, which exhibited satisfactory results.

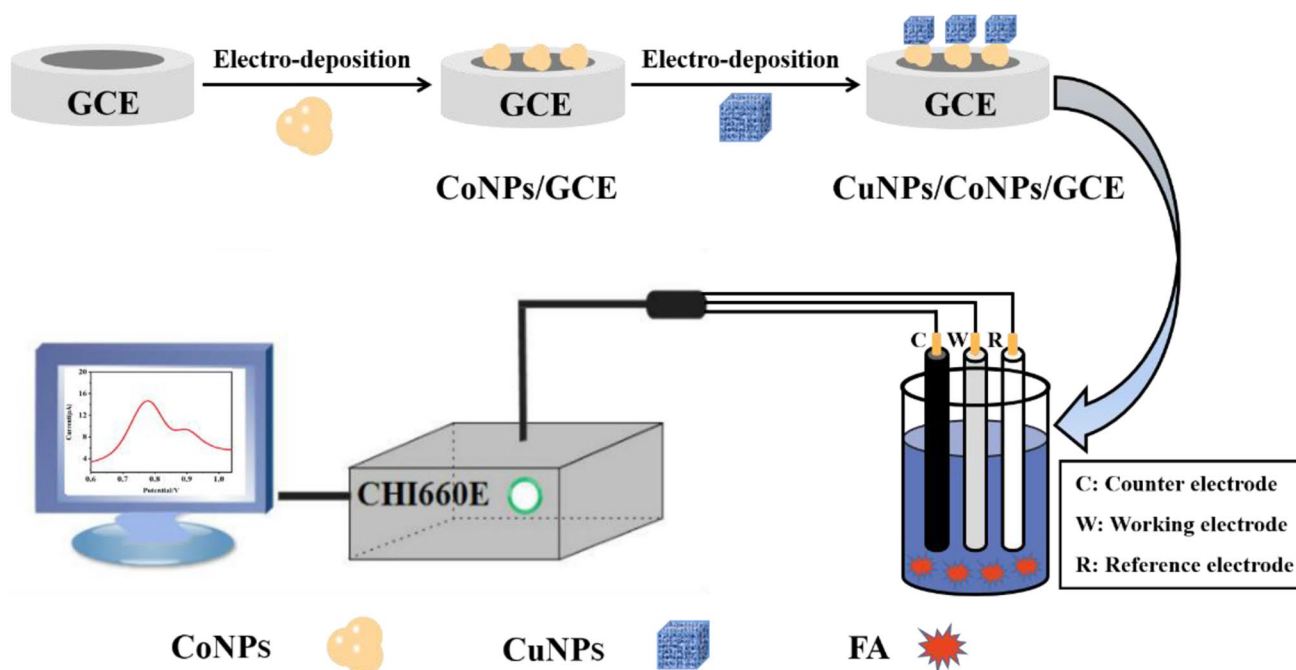
Experimental section

Reagents and materials

Thiophene, indole, pyrrole, and dopamine (DA) were purchased from MacLin Biochemical Technology Co., Ltd. (Shanghai, China). $CoCl_2 \cdot 6H_2O$, $CuSO_4 \cdot 5H_2O$, H_2PtCl_6 and $AgNO_3$ were purchased from Shanghai Changxi Biotechnology Co., Ltd. (Shanghai, China). Folic acid (FA) was obtained from Aladdin Reagent Co., Ltd. (Shanghai, China). FA tablets (0.4 mg per tablet) were obtained from a local supermarket (Guilin, China). Phosphate buffer solution (PBS, 0.2 M) was prepared with Na_2HPO_4 and NaH_2PO_4 as electrolyte, and the pH was adjusted according to the mixed ratio. Distilled water was used to prepare the reagents, which were all of analytical grade.

Instruments and apparatus

A CHI660E electrochemical workstation (Shanghai Chenhua Instruments Co., Ltd, Shanghai, China) was used for all tests with a glassy carbon electrode (GCE, $\phi=3$ mm) as the working electrode, platinum wire as the counter electrode, and Ag/AgCl (in saturated KCl) as the reference electrode, respectively. All reagents were ultrasonically dissolved using an SK1200B ultrasonic cleaner (Shanghai Kudos Ultrasonic Instrument Co., Ltd, China) at 35 kHz. DPV was carried out with a pulse amplitude of 0.05 V and a pulse width of 0.06 s. Amperometry ($i-t$) was used for electrodeposition and selectivity study. All electrochemical impedance spectroscopy (EIS) measurements were performed with a frequency range from 100,000 to 0.1 Hz with the open-circuit potential as an initial voltage in 5.0 mM ferricyanide and ferrocyanide solution ($K_3[Fe(CN)_6]$ and $K_4[Fe(CN)_6]$). The morphology and energy spectrum were



Scheme 2 Formulation of a CuNPs/CoNPs/GCE electrochemical sensor for detection of FA

obtained using a field emission scanning electron microscope (Hitachi SU8020, Japan) with an acceleration voltage ranging from 0.5 to 30 kV and an X-ray energy resolution of 130 eV, respectively.

Electrode modification and detection of FA

A 10.0 mM FA solution was prepared by dissolving FA reagent in 0.2 M PBS (pH 7.0), and was sealed and stored in a refrigerator at 4 °C. Later, thiophene, indole and pyrrole were dissolved to 10.0 mM in anhydrous ethanol. Then, 10.0 mM DA, CoCl₂, CuSO₄, H₂PtCl₆ and AgNO₃ were prepared in ultrapure water and stored at 4 °C. All GCEs were polished with 1.0, 0.5 and 0.3 μm alumina powder, then ultrasonically cleaned and activated in 0.5 M H₂SO₄ by cyclic voltammetry (CV) from −0.20 to +1.20 V for 20 cycles.

Firstly, through the *i-t* method, bare GCEs were modified by active materials (thiophene, indole, pyrrole and DA) with an initial voltage of 0.10 V for 400 s and metal NPs (CoNPs, CuNPs, AgNPs, and PtNPs) with an initial voltage of −0.50 V for 100 s, respectively. Secondly, the order of modifiers, including CuNPs then CoNPs, CoNPs then CuNPs and a mixture of CuNPs and CoNPs, was also deposited on GCE by the *i-t* method with an initial voltage of −0.50 V for 100 s.

The constructed electrodes were characterized by EIS, SEM and EDS. The electrodeposition potential, time, pH,

temperature and other related experimental parameters were optimized. Under the optimum conditions, the linear relationship, repeatability and stability of the prepared sensor were studied. First, 100 μL 10.0 mM FA, glucose (Glc), biotin, DA and glutamic acid (Glu) were dropped into 3.0 mL PBS at intervals of 50 s with the *i-t* method applied. The facile preparation of the CuNPs/CoNPs/GCE electrochemical sensor used for the detection of FA through DPV is shown in Scheme 2.

Results and discussion

Properties of electrodes modified with different active materials

Firstly, bioactive materials usually have different electrocatalytic properties for FA [38, 39]. Four sensors modified with thiophene, indole, pyrrole, and DA were tested in PBS (pH 7.0), and the obtained DPV curves are shown in Fig. S1a. As shown, curve a is a smooth straight line, which indicates that no electrochemical reaction occurred on the bare GCE. However, curves b, c, d, and e exhibit distinct peaks at +0.32, +0.53, +0.65 or +0.94 V, respectively, which indicates that all active substances were deposited on bare GCEs. Additionally, Fig. S1b demonstrates that the four active substances

had different catalytic effects on FA. Figure S1b shows the DPV response of the bare GCE and GCEs modified by thiophene, indole, pyrrole, and DA in 1 mM FA. The modified electrodes in Fig. S1b all have characteristic peaks near +0.80 V. It is worth noting that the shape and height of the response peak on the left is more prominent than that on the right, although their peak currents were all less than 4.0 μA . Furthermore, compared with the bare GCE, GCEs modified with active substance (curves b, c, d, e) had a slight increase in the current response value, demonstrating that the four active substances have different electrocatalytic abilities for FA.

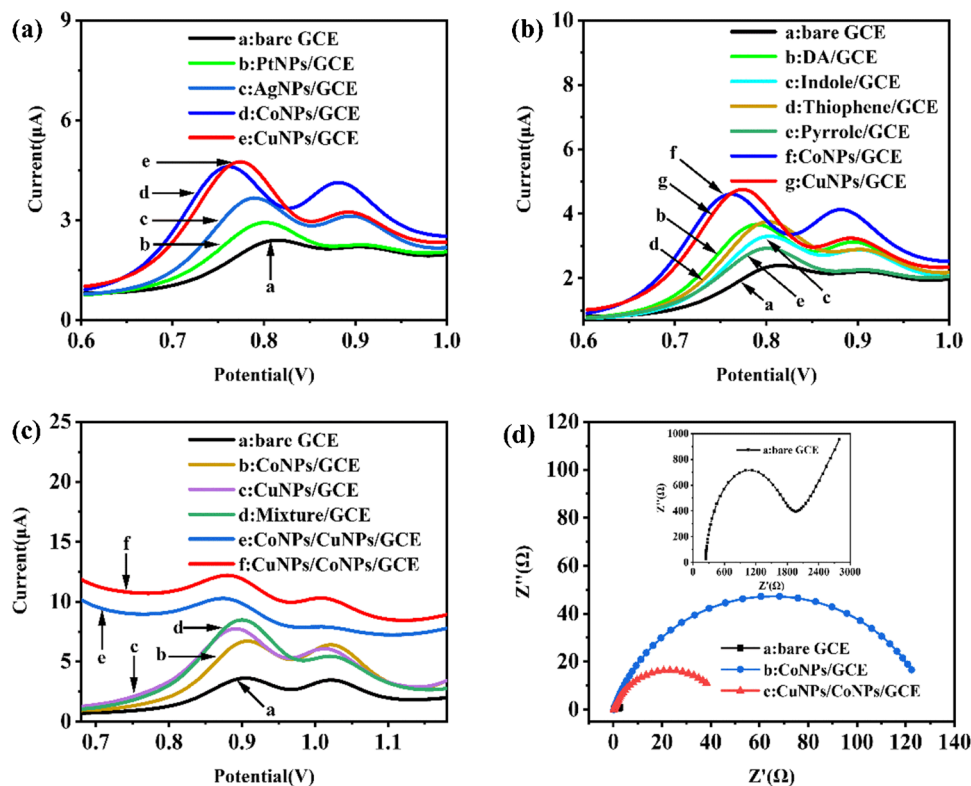
Properties of electrodes modified with different metal NPs

Monometallic NPs can amplify response signal because of their special shape and size properties and high electronic conductivity [40–42]. In this work, GCEs modified with four monometallic NPs, including PtNPs, AgNPs, CoNPs and CuNPs, were compared and selected. As the result of the experiment, the DPV response of GCEs modified by PtNPs, AgNPs, CoNPs, and CuNPs in PBS at pH 7.0 is shown in Fig. S2, respectively. Curve a is practically a smooth straight line, which illustrates that no electrochemical reaction occurred on the bare GCE. Curves b, c and e

all show distinct characteristic peaks at -0.05 , $+0.05$ or $+0.18$ V, respectively. However, curve d lacks a distinct characteristic peak. The different characteristic peaks indicate that all monometallic NPs were deposited on the GCE. Furthermore, in Fig. 1a, FA was catalyzed by bare GCE, PtNPs/GCE, AgNPs/GCE, CoNPs/GCE, and CuNPs/GCE, respectively. The modified electrodes in Fig. 1a had similar characteristic peaks near $+0.80$ and $+0.90$ V. The peak current values of curves d and e were not significantly different, although they were both less than 6.00 μA .

Furthermore, compared to bare GCE, the characteristic peak current of the four monometallic NP-modified electrodes was increased and varied, which indicated that the four monometallic NPs had different effects on FA because of their specific surface area and low impedance. Interestingly, in Fig. 1b, the left peak current value was ordered as curve g (4.80 μA) > curve f (4.60 μA) > curve e (3.70 μA) > curve d (3.60 μA) > curve c (3.30 μA) > curve b (2.90 μA) > curve a (2.40 μA), indicating that the GCEs modified by CoNPs and CuNPs in Fig. 1b had higher peak current values than GCEs modified by either bioactive material. Hence, CoNPs and CuNPs were chosen as the monometallic materials to be modified on GCEs. Moreover, compared with the characteristic peak on the right, the characteristic peak on the left side had a more prominent shape and height in the subsequent experiment. Consequently, it deserves attention in subsequent experimental analysis.

Fig. 1 **a** The different metal NP-modified GCEs in 1.00 mM FA (a, bare GCE; b, PtNPs/GCE; c, AgNPs/GCE; d, CoNPs/GCE; e, CuNPs/GCE). **b** The different sensors were detected in 1 mM FA (a, bare GCE; b, DA/GCE; c, indole/GCE; d, thiophene/GCE; e, pyrrole/GCE; f, CoNPs/GCE; g, CuNPs/GCE). **c** Sensors modified by different depositional way and order in 1.25 mM FA (a, bare GCE; b, CoNPs/GCE; c, CuNPs/GCE; d, Mixture/GCE; e, CoNPs/CuNPs/GCE; f, CuNPs/CoNPs/GCE). **d** EIS curves of different modified electrodes (a, bare GCE; b, CoNPs/GCE; c, CuNPs/CoNPs/GCE) in 5.0 mM $[\text{Fe}(\text{CN})_6]^{3-/4-}$ containing 0.1 M KCl



In addition, bimetallic NPs generally have higher conductivity, larger specific surface area and higher electrocatalytic properties than monometallic NPs [43, 44]. Hence, the depositional way and order were explored by DPV, and the results are shown in Fig. 1c. A mixture of CuNPs and CoNPs (curve c), CoNPs then CuNPs (curve e), CuNPs then CoNPs (curve f) were electrodeposited on GCEs by the *i-t* method, respectively. The left peak current value near +0.90 V was ordered as follows: f (12.20 μ A) > e (10.30 μ A) > d (8.50 μ A) > c (7.70 μ A) > b (6.70 μ A) > a (3.60 μ A), respectively. Compared with the other curves, curve f had the largest left

characteristic peak current value. Interestingly, the characteristic peak current value of curve f (12.20 μ A) on the left side was nearly twice as high as curve b (6.70 μ A) and curve c (7.70 μ A), and four times as high as curve a (3.60 μ A). Hence, compared with monometallic NPs (CoNPs, CuNPs), bimetallic NPs (CuNPs/CoNPs) synergistically amplified the response signal of FA [45]. The deposition order was first deposited CoNPs and then deposited CuNPs.

Moreover, the EIS results of bare GCE (a), CoNPs/GCE (b), and CuNPs/CoNPs/GCE (c) are shown in Fig. 1d. Based on the Randles equivalent circuit [22], the electron

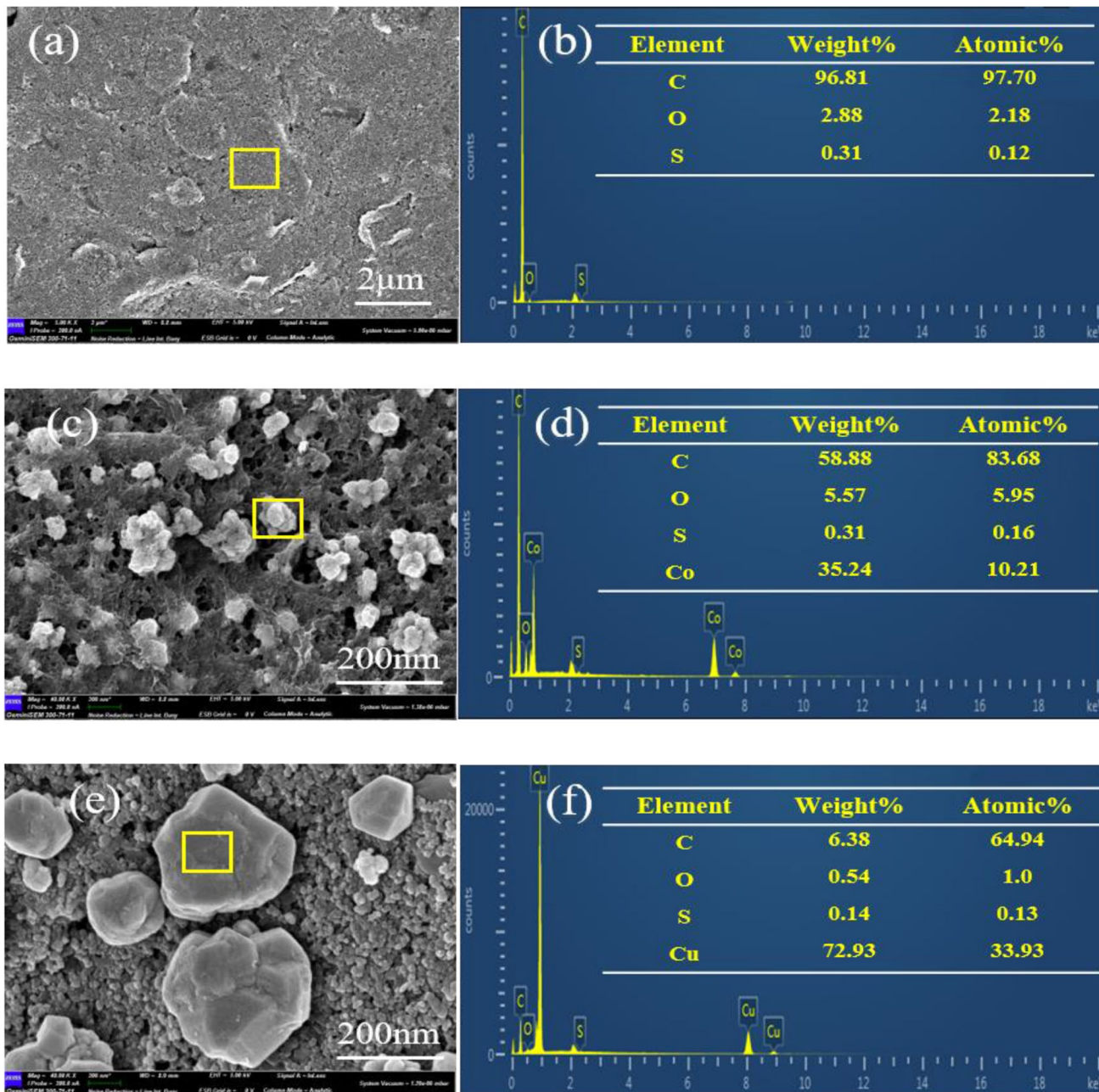


Fig. 2 SEM and EDS of different modified electrodes (a, b: bare SPCE; c, d: CoNPs/SPCE; e, f: CuNPs/CoNPs/SPCE). The sampling points of EDS are indicated in the yellow box in the SEM

transfer resistance (R_{ct}) of bare GCE (curve a), CoNPs/GCE (curve b) and CuNPs/CoNPs/GCE (curve c) are calculated as 0.20 k Ω , 122.40 k Ω , 38.20 k Ω , respectively. It is noteworthy that the R_{ct} of CoNPs/GCE was much greater than CoNPs, CuNPs, and bimetallic NPs (CuNPs then CoNPs) reduced the impedance and accelerated the electron transport efficiency as its synergistic amplification effect [46]. Similarly, the same result also proved that the CuNPs/CuNPs/GCE sensor was successfully constructed, which is consistent with the SEM results.

Characterization of the sensor by SEM and EDS

The success of the various steps of electrode modification was demonstrated and verified by surface morphology and element distribution characterization. Screen-printed carbon electrodes (SPCE) were used for the modification in this section, instead of GCE. SEM and EDS of bare SPCE (a, b), CoNPs/SPCE (c, d), and CuNPs /CoNPs/SPCE (e, f) are shown in Fig. 2. The sampling points of EDS are indicated in the yellow box in the SEM. As shown in Fig. 2a, the surface of SPCE was relatively flat, and the corresponding EDS (Fig. 2b) showed that the bare SPCE contained a large amount of C (97.1wt%), as expected. Figure 2c shows generous irregular flower-shaped particles, and the corresponding Fig. 2d demonstrates the presence of large amounts of C and Co (58.88 wt% and 35.24 wt%). Figure 2e shows massive particles of diverse sizes, and Fig. 2f shows the presence of Cu and C (72.93 wt% and 6.38 wt%). It is worth noting that Co does not appear on the electrode in Fig. 2f, which may be due to the complete coverage of the later electrodeposited CuNPs, and the signal of Co may be completely covered by the signal of the extensive Cu. This result is consistent with previous EIS results and demonstrated in subsequent experiments. Apparently, the results of SEM and EDS indicate that the CuNPs/CoNPs/SPCE were successfully constructed.

Optimization study

The constructed sensors were studied under different experimental conditions in Fig. S3, including deposition voltage and time, pH value for FA quantification, and ambient temperature. The sensors modified with the metal nanolayer were determined by the deposition potential and deposition time of metal NPs, which directly affect the detection results of FA. First, in Fig. S3a, the deposition voltage of CoNPs was set to -0.70 , -0.50 , -0.30 , -0.10 , $+0.10$, and $+0.30$ V, respectively, while all other experimental conditions remained constant. Compared with other curves, curve e in Fig. S3a was the highest current value on the left side. This may be due to the decrease of the impedance of

the sensor and the increase of the electron transfer rate as the CoNPs were deposited on the GCE, which was consistent with the EIS results. The peak current value on the left side decreased as the deposition voltage increased except -0.70 V, indicating that with the enrichment of CoNPs, the sensor working surface may become thicker, resulting in an impedance increase and further reducing the signal amplification effect. As a result, -0.50 V was selected as the optimized voltage for CoNPs deposition. The deposition time was also set to 20, 50, 80, 105, 145 and 190 s by the i - t method, respectively. In Fig. S3b, the deposition time increased from 35 to 105 s, and the response current value of FA increased, which means that many more CoNPs were electrodeposited, while the deposition time increased from 105 to 190 s and the response current value of FA decreased, which means that with the increase in the deposition time of CoNPs, the enrichment of CoNPs led to a decrease in the signal amplification effect. As a consequence, the deposition time for the CoNPs was set as 105 s.

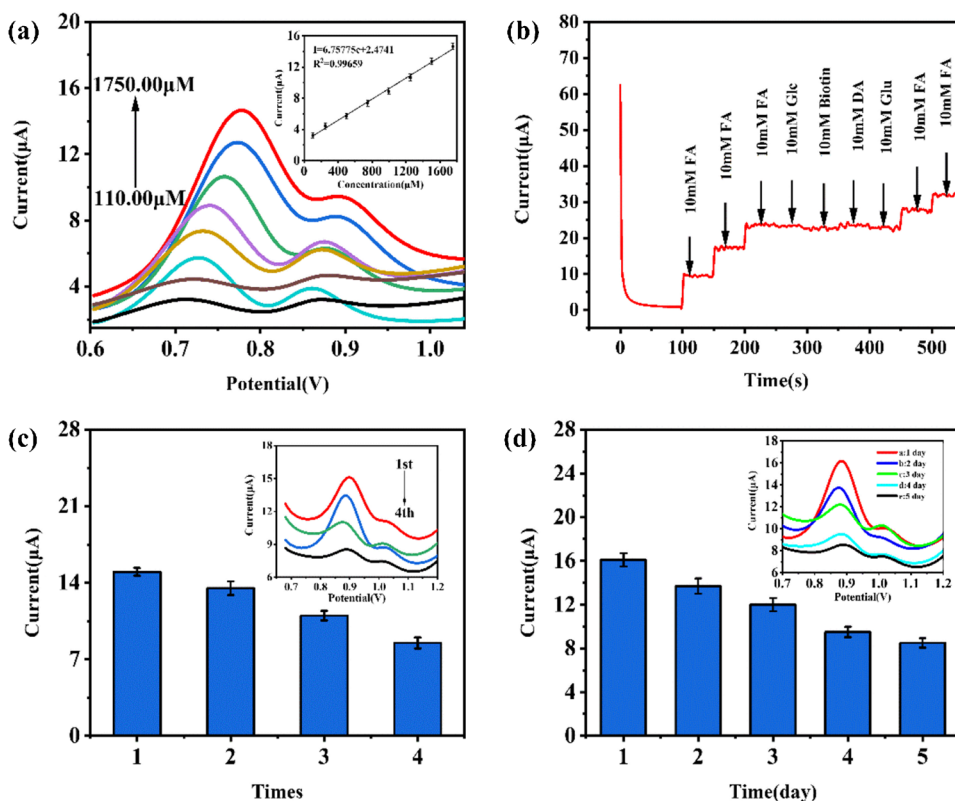
Likewise, in Fig. S3c, the deposition voltage of CuNPs was set to -0.70 , -0.50 , -0.30 , -0.10 , $+0.10$, and $+0.30$ V, respectively. The peak current value on the left side decreased as the deposition voltage increased except -0.50 V. As a result, -0.50 V was selected as the optimized voltage for CuNP deposition. Then, the deposition time of CuNPs was also set to 15, 50, 70, 85, 110, and 140 s by the i - t method, respectively. The peak current value of curve b was the largest in Fig. S3d, and it decreased as deposition time increased. The deposition time of CuNPs was set as 50 s. With the increase of deposition voltage and time of CuNPs, FA response current increased first and then decreased, which may be due to the enrichment of CuNPs, and the working surface of the sensor may become thicker, resulting in the increase of its impedance and further reducing the signal amplification effect.

After that, the effects of the target solution pH and temperature on FA detection were studied. The left peak value in the neutral and basic solution of FA had higher than the acidic solution in Fig. S3e, and the current value was highest at pH 7.0. This result could be explained by the fact that FA is unstable and easily destroyed in an acidic environment. Hence, pH 7.0 was chosen for FA quantitation. Moreover, the peak current gradually increased from 4 to 25 °C, but decreased from 25 to 35 °C as shown in Fig. S3f. Thus, the subsequent experiments were performed at 25 °C.

FA detection

Figure 3a shows DPVs of FA at different concentrations from 110.00 to 1750.00 μ M with CuNPs/CoNPs/GCE.

Fig. 3 **a** Relative responses of CuNPs/CoNPs/GCE with different concentrations of FA from 110.00, 250.00, 500.00, 750.00, 1000.00, 1250.00, 1500.00, 1750.00 μM at 25 $^{\circ}\text{C}$, pH 7.0 (Inset: linear regression equation between anodic peak currents and concentrations of FA). The selectivity (**b**), repeatability (**c**) and stability (**d**) of the sensor for FA at 25 $^{\circ}\text{C}$, pH 7.0, respectively



(Inset: the linear relationship between peak anode current and FA concentration). Selectivity, repeatability, and stability studies are shown in Fig. 3b, c and d, respectively.

Firstly, the different concentrations of FA were measured by DPV. As shown in Fig. 3a, the peak current value on the left increased gradually as the FA concentration increased. The left peak current I (μA) and concentration c (μM) showed a good linear relationship between 110.00 and 1750.00 μM , $I = 6.75775c + 2.4741$, with a limit of detection (LOD) of 30.584 μM and sensitivity of 95.72 $\mu\text{A mM}^{-1}\text{cm}^{-2}$. Surprisingly, the CuNPs/CoNPs/GCE sensor had a wide detection range when compared to the other methods in Table S1. In comparison to the complexity of other sensors, the sensor had the significant advantage of easy preparation.

Secondly, the selectivity of the CuNPs/CoNPs/GCE sensor was evaluated by measuring the $i-t$ response current after adding different interferences in PBS (pH 7.0) every 50 s. Throughout the experiment, the mixed solution was uniformly dispersed by a magnetic stirrer. After gradually adding three drops of 100 μL 10.00 mM FA, the current value increased first and then stabilized, as shown in Fig. 3b. As 10.00 mM Glc, biotin, DA, and Glu dropped, the current remained relatively stable. The current was gradually increased after two further dropping of FA solution. Hence, the sensor had a good selectivity.

Next, the repeatability of CuNPs/CoNPs/GCE sensor was assessed. The CuNPs/CoNPs/GCE sensor was continuously tested four times by DPV in FA solution with the same concentration. Peak current values showed a gradual decrease and a linear gradient, as shown in Fig. 3c. This may be due to the enrichment of electrochemical reaction products on the interface, resulting in the reduction of the available reaction site. As a consequence, continuous multiple detection would be not possible with the CuNPs/CoNPs/GCE sensors.

Finally, the stability of the sensor was tested in Fig. 3d. The same concentration of FA was detected at different time points under the same conditions (25 $^{\circ}\text{C}$, pH 7.0) by CuNPs/CoNPs/GCE. In the first 3 days, the current response values were relatively stable, but on the fourth and fifth days, the current response values gradually declined.

Table 1 The detection of FA in tablet samples by the sensor ($n=3$)

Spiked (μM)	Differential current ΔI (μA)	Average found (μM)	Recovery (%)	RSD (%)
0	3.93 \pm 0.78	214.99 \pm 115.48	-	8.00
220.00	5.44 \pm 0.39	438.39 \pm 57.32	101.54	2.87
440.00	7.07 \pm 0.12	680.53 \pm 17.43	110.06	0.67
660.00	8.44 \pm 1.19	882.43 \pm 175.49	91.77	5.66

Analysis of real samples

Four sample solutions of the same concentration were prepared by crushing and dissolving FA tablets in 0.2 M PBS at pH 7.0. All spiked samples were tested three times using the standard addition method, and the results are shown in Table 1. The recovery of the constructed sensor was from 91.77 to 110.06 %, indicating that the sensor had potential applications in detecting FA tablets.

Conclusions

In summary, we fabricated a CuNPs/CoNPs/GCE sensor for FA detection with a simple, low-cost, and sensitive process. A bimetallic CuNPs/CoNPs layer was formed by simple step-by-step electrodeposition. Interestingly, the response current of a sensor modified by CuNPs/CoNPs is nearly twice as high as a sensor modified by CuNPs or CoNPs because CuNPs/CoNPs reduce the impedance, may increase the specific surface area and site of the reaction, and have a synergistic amplification effect on the FA response signal. The results showed that the sensor exhibited an excellent linear relationship over a wide range of 110.00–1750.00 μM with a LOD of 34.79 μM , and Glc, biotin, DA, and Glu interfered only slightly with FA detection. Furthermore, the sensor can be used for the detection of FA tablets for its satisfactory selectivity and stability, with an average recovery rate of 91.77–110.06%.

Supplementary Information The online version contains supplementary material available at <https://doi.org/10.1007/s00216-022-04242-w>.

Acknowledgments We appreciate the financial support from the National Natural Science Foundation of China (No.61661014, 81873913, 61861010, 61627807), the Natural Science Foundation of Guangxi Province (No. 2018GXNSFAA281198, 2018GXNS-FBA281135), Guangxi One Thousand Young and Middle-aged College and University Backbone Teachers Cultivation Program and Guangxi Colleges and Universities Key Laboratory of Biomedical Sensors and Intelligent Instruments. Funding from the Natural Science and Engineering Research Council of Canada and the University of Toronto are appreciated.

Declarations

Conflict of interest The authors declare no competing interests.

References

- Di Tinno A, Cancelliere R, Micheli L. Determination of folic acid using biosensors—a short review of recent progress. *Sensors*. 2021;21(10):3360. <https://doi.org/10.3390/s21103360>.
- Bulloch RE, Wall CR, McCowan LME, Taylor RS, Roberts CT, Thompson JMD. The effect of interactions between folic acid supplementation and one carbon metabolism gene variants on small-for-gestational-age births in the screening for pregnancy endpoints (scope) cohort study. *Nutrients*. 2020;12(6):1677. <https://doi.org/10.3390/nu12061677>.
- Jouanne M, Oddoux S, Noel A, Voisin-Chiret AS. Nutrient requirements during pregnancy and lactation. *Nutrients*. 2021;13(2):692. <https://doi.org/10.3390/nu13020692>.
- Svaton M, Kramarzova KS, Kanderova V, Mancikova A, Smisek P, Jesina P, et al. A homozygous deletion in the SLC19A1 gene as a cause of folate-dependent recurrent megaloblastic anemia. *Blood*. 2020;135(26):2427–31. <https://doi.org/10.1182/blood.2019003178>.
- Li Y, Spence JD, Wang X, Huo Y, Xu X, Qin X. Effect of vitamin B-12 levels on the association between folic acid treatment and ckd progression: A post hoc analysis of a folic acid interventional trial. *Am J Kidney Dis*. 2020;75(3):325–32. <https://doi.org/10.1053/j.ajkd.2019.07.020>.
- Puga AM, Ruperto M, de Lourdes S-VM, Montero-Bravo A, Partearroyo T, Varela-Moreiras G. Effects of supplementation with folic acid and its combinations with other nutrients on cognitive impairment and alzheimer's disease: A narrative review. *Nutrients*. 2021;13(9):2966. <https://doi.org/10.3390/nu13092966>.
- Cheng M, Yang L, Dong Z, Wang M, Sun Y, Liu H, et al. Folic acid deficiency enhanced microglial immune response via the notch1/nuclear factor kappa B p65 pathway in hippocampus following rat brain I/R injury and BV2 cells. *J Cell Mol Med*. 2019;23(7):4795–807. <https://doi.org/10.1111/jcmm.14368>.
- Wiens D, DeSoto MCJBs. Is high folic acid intake a risk factor for autism?—a review. *Brain Sci*. 2017;7(11):149. <https://doi.org/10.3390/brainsci7110149>.
- Kang L, Lin C, Ning F, Sun X, Zhang M, Zhang H, et al. Rapid determination of folic acid and riboflavin in urine by polypyrrole magnetic solid-phase extractant combined ultra-performance liquid chromatography. *J Chromatogr A*. 2021;1648:462192. <https://doi.org/10.1016/j.chroma.2021.462192>.
- Zhu T, Wang H, Zang L, Jin S, Guo S, Park E, et al. Flexible and reusable ag coated TiO₂ nanotube arrays for highly sensitive sers detection of formaldehyde. *Molecules*. 2020;25(5):1199. <https://doi.org/10.3390/molecules25051199>.
- Cao Y, Griffith B, Bhomkar P, Wishart DS, McDermott MTJA. Functionalized gold nanoparticle-enhanced competitive assay for sensitive small-molecule metabolite detection using surface plasmon resonance. *Analyst*. 2018;143(1):289–96. <https://doi.org/10.1039/c7an01680h>.
- Sharma A, Arya S. Economical and efficient electrochemical sensing of folic acid using a platinum electrode modified with hydrothermally synthesized Pd and Ag Co-doped SnO₂ nanoparticles. *J Electrochem Soc*. 2019;166(13):B1107. <https://doi.org/10.1149/2.0261913jes>.
- Han G-C, Li H, Ferranco A, Zhan T, Cheng Y, Chen Z, et al. The construction of a simple sensor for the simultaneous detection of nitrite and thiosulfate by heme catalysis. *RSC Adv*. 2020;10(58):35007–16. <https://doi.org/10.1039/D0RA06942F>.
- Safaei M, Beitollahi H, Shishehbore MR. Amplified electrochemical sensor employing Fe₃O₄@SiO₂/graphene nanocomposite for selective determination of folic acid. *J Anal Chem*. 2020;75(1):95–100. <https://doi.org/10.1134/s1061934820010141>.
- Zhan T, Feng X-Z, An Q-Q, Li S, Xue M, Chen Z, et al. Enzyme-free glucose sensors with efficient synergistic electro-catalysis based on a ferrocene derivative and two metal nanoparticles. *RSC Adv*. 2022;12(9):5072–9. <https://doi.org/10.1039/D1RA09213H>.

16. An Q-Q, Feng X-Z, Zhou Z-F, Zhan T, Lian S-F, Zhu J, et al. One step construction of an electrochemical sensor for melamine detection in milk towards an integrated portable system. *Food Chem.* 2022;383:132403. <https://doi.org/10.1016/j.foodchem.2022.132403>.
17. Dokur E, Gorduk O, Sahin Y. Differential pulse voltammetric determination of folic acid using a poly(cystine) modified pencil graphite electrode. *Anal Lett.* 2020;53(13):2060–78. <https://doi.org/10.1080/00032719.2020.1728540>.
18. Zhan T, Feng X-Z, Cheng Y, Han G-C, Chen Z, Kraatz H-B. Synergistic electrochemical amplification of ferrocene carboxylic acid nanoflowers and cu nanoparticles for folic acid sensing. *J Electrochem Soc.* 2022;169(7):077510. <https://doi.org/10.1149/1945-7111/ac8022>.
19. Batra B, Narwal V, Kalra V, Sharma M, Rana JS. Folic acid biosensors: A review. *Process Biochem.* 2020;92:343–54. <https://doi.org/10.1016/j.procbio.2020.01.025>.
20. Khan SI, Tadi KK, Chillawar RR, Motghare RV. Interfacing electrochemically reduced graphene oxide with poly(erichrome black T) for simultaneous determination of epinephrine, uric acid and folic acid. *J Electrochem Soc.* 2018;165(16):B804. <https://doi.org/10.1149/2.0121816jes>.
21. Joshi A, Kim K-H. Recent advances in nanomaterial-based electrochemical detection of antibiotics: Challenges and future perspectives. *Biosens.* 2020;153:112046. <https://doi.org/10.1016/j.bios.2020.112046>.
22. Yuan M-M, Zou J, Huang Z-N, Peng D-M, Yu J-G. PtNPs-GNPs-MWCNTs- β -Cd nanocomposite modified glassy carbon electrode for sensitive electrochemical detection of folic acid. *Anal Bioanal Chem.* 2020;412(11):2551–64.
23. Elumalai S, Mani V, Jeromiyas N, Ponnusamy VK, Yoshimura M. A composite film prepared from titanium carbide $Ti_3C_2T_x$ (MXene) and gold nanoparticles for voltammetric determination of uric acid and folic acid. *Microchim Acta.* 2020;187(1):1–10. <https://doi.org/10.1007/s00604-019-4018-0>.
24. Han G-C, Su X, Hou J, Ferranco A, Feng X-Z, Zeng R, et al. Disposable electrochemical sensors for hemoglobin detection based on ferrocenyl cysteine conjugates modified electrode. *Sens Actuators B: Chem.* 2019;282:130–6. <https://doi.org/10.1016/j.snb.2018.11.042>.
25. Liu J-G, Wan J-Z, Lin Q-M, Han G-C, Feng X-Z, Chen Z. Convenient heme nanorod modified electrode for quercetin sensing by two common electrochemical methods. *Micromachines.* 2021;12(12):1519. <https://doi.org/10.3390/mi12121519>.
26. Feng X-Z, Li H, Ferranco A, Chen Z, Xue M, Han G-C, et al. A very simple method for detection of bisphenol a in environmental water by heme signal amplification. *J Electrochem Soc.* 2020;167(6). <https://doi.org/10.1149/1945-7111/ab7e20>.
27. Yang Z, Gong F, Yu Z, Shi D, Liu S, Chen M. Highly sensitive folic acid colorimetric sensor enabled by free-standing molecularly imprinted photonic hydrogels. *Polym Bull.* 2022;79(3):1857–71. <https://doi.org/10.1007/s00289-021-03584-2>.
28. Wang Q, Xiao X, Hu X, Huang L, Li T, Yang M. Molecularly imprinted electrochemical sensor for ascorbic acid determination based on mxene modified electrode. *Mater Lett.* 2021;285:129158. <https://doi.org/10.1016/j.matlet.2020.129158>.
29. Garcia SM, Wong A, Khan S, Sotomayor MDPT. A simple, sensitive and efficient electrochemical platform based on carbon paste electrode modified with Fe_3O_4 @MIP and graphene oxide for folic acid determination in different matrices. *Talanta.* 2021;229. <https://doi.org/10.1016/j.talanta.2021.122258>.
30. Bettazzi F, Ingrosso C, Sfragano PS, Pifferi V, Falciola L, Curri ML, et al. Gold nanoparticles modified graphene platforms for highly sensitive electrochemical detection of vitamin C in infant food and formulae. *Food Chem.* 2021;344. <https://doi.org/10.1016/j.foodchem.2020.128692>.
31. Wong A, Santos AM, Silva TA, Fatibello-Filho OJT. Simultaneous determination of isoproterenol, acetaminophen, folic acid, propranolol and caffeine using a sensor platform based on carbon black, graphene oxide, copper nanoparticles and pedot: Pss. *Talanta.* 2018;183:329–38. <https://doi.org/10.1016/j.talanta.2018.02.066>.
32. Tefera M, Tessema M, Admassie S, Ward M, Phelane L, Iwuoha EI, et al. Electrochemical application of cobalt nanoparticles-polypyrrole composite modified electrode for the determination of phoxim. *Analytica chimica acta: X.* 2021;9:100077. <https://doi.org/10.1016/j.acax.2021.100077>.
33. Park C, Koo WT, Chong S, Shin H, Kim YH, Cho HJ, et al. Confinement of ultrasmall bimetallic nanoparticles in conductive metal-organic frameworks via site-specific nucleation. *Adv Mater.* 2021;33(38):2101216. <https://doi.org/10.1002/adma.202170302>.
34. Park CE, Lee H, Senthil RA, Jeong GH, Choi MY. Bimetallic nickel-palladium nanoparticles with low Ni content and their enhanced ethanol oxidation performance: Using a pulsed laser as modification machinery. *Fuel.* 2022;321:124108. <https://doi.org/10.1016/j.fuel.2022.124108>.
35. Liu Y, Yao S, Hu G, Ye Y, Wang H. In-situ electrochemical co-deposition of bimetallic CuCo nanoparticles on cubic mesoporous carbon for ultrasensitive electrochemical sensing of cyadox. *Electrochim Acta.* 2021;380:138128. <https://doi.org/10.1016/j.electacta.2021.138128>.
36. Wang Q, Si H, Zhang L, Li L, Wang X, Wang SJACA. A fast and facile electrochemical method for the simultaneous detection of epinephrine, uric acid and folic acid based on ZrO_2/ZnO nanocomposites as sensing material. *Anal Chim Acta.* 2020;1104:69–77. <https://doi.org/10.1016/j.aca.2020.01.012>.
37. Tajik S, Beitollahi H, Shahsavari S, Nejad FGJC. Simultaneous and selective electrochemical sensing of methotrexate and folic acid in biological fluids and pharmaceutical samples using Fe_3O_4 /ppy/Pd nanocomposite modified screen printed graphite electrode. *Chemosphere.* 2022;291:132736. <https://doi.org/10.1016/j.chemosphere.2021.132736>.
38. Roman G, Pappas AC, Kovala-Demertzi D, Prodromidis MI. Preparation of a 2-(4-fluorophenyl)indole-modified xerogel and its use for the fabrication of screen-printed electrodes for the electrocatalytic determination of sulfide. *Anal Chim Acta.* 2004;523(2):201–7. <https://doi.org/10.1016/j.aca.2004.07.037>.
39. Cheng S, Tang D, Zhang Y, Xu L, Liu K, Huang K, et al. Specific and sensitive detection of tartrazine on the electrochemical interface of a molecularly imprinted polydopamine-coated PtCo nanoalloy on graphene oxide. *Biosens.* 2022;12(5):326. <https://doi.org/10.3390/bios12050326>.
40. Cheng S, Liu H, Zhang H, Chu G, Guo Y, Sun XJS, et al. Ultrasensitive electrochemiluminescence aptasensor for kanamycin detection based on silver nanoparticle-catalyzed chemiluminescent reaction between luminol and hydrogen peroxide. *Sens Actuators B: Chem.* 2020;304:127367. <https://doi.org/10.1016/j.snb.2019.127367>.
41. Suresh L, Bondili J, Brahman PJMTC. Development of proof of concept for prostate cancer detection: An electrochemical immunosensor based on fullerene- C_{60} and copper nanoparticles composite film as diagnostic tool. *Mater Today Chem.* 2020;16:100257. <https://doi.org/10.1016/j.mtchem.2020.100257>.
42. Zhang R, Fu K, Zou F, Bai H, Zhang G, Liang F, et al. Highly sensitive electrochemical sensor based on pt nanoparticles/carbon nanohorns for simultaneous determination of morphine and mdma in biological samples. *Electrochim Acta.* 2021;370:137803. <https://doi.org/10.1016/j.electacta.2021.137803>.

43. Su L, Cheng Y, Shi J, Wang X, Xu P, Chen Y, et al. Electrochemical sensor with bimetallic Pt-Ag nanoparticle as catalyst for the measurement of dissolved formaldehyde. *J Electrochem Soc.* 2022;169(4):047507.
44. Sun X, Wang N, Xie Y, Chu H, Wang Y, Wang YJT. In-situ anchoring bimetallic nanoparticles on covalent organic framework as an ultrasensitive electrochemical sensor for levodopa detection. *Talanta.* 2021;225:122072. <https://doi.org/10.1016/j.talanta.2020.122072>.
45. Ge S, Zhang Y, Zhang L, Liang L, Liu H, Yan M, et al. Ultrasensitive electrochemical cancer cells sensor based on trimetallic dendritic Au@PtPd nanoparticles for signal amplification on lab-on-paper device. *Sens Actuators B: Chem.* 2015;220:665–72. <https://doi.org/10.1016/j.snb.2015.06.009>.
46. Cheng Y-Y, Zhan T, Feng X-Z, Han G-C. A synergistic effect of gold nanoparticles and melamine with signal amplification for C-reactive protein sensing. *J Electroanal Chem.* 2021;895:115417. <https://doi.org/10.1016/j.jelechem.2021.115417>.

Publisher's note Springer Nature remains neutral with regard to jurisdictional claims in published maps and institutional affiliations.

Springer Nature or its licensor holds exclusive rights to this article under a publishing agreement with the author(s) or other rightsholder(s); author self-archiving of the accepted manuscript version of this article is solely governed by the terms of such publishing agreement and applicable law.